

Online Battery Equivalent Circuit Model Estimation on Continuous-Time Domain Using Linear Integral Filter Method

Cheng Zhang, James Marco, Walid Allafi, Truong Q. Dinh, W. D. Widanage

Abstract—Equivalent circuit models (ECMs) are widely used in battery management systems in electric vehicles and other battery energy storage systems. The battery dynamics and the model parameters vary under different working conditions, such as different temperature and state of charge (SOC) levels, and therefore online parameter identification can improve the modelling accuracy. This paper presents a way of online ECM parameter identification using a continuous time (CT) estimation method. The CT estimation method has several advantages over discrete time (DT) estimation methods for ECM parameter identification due to the widely separated battery dynamic modes and fast sampling. The presented method can be used for online SOC estimation. Test data are collected using a lithium ion cell, and the experimental results show that the presented CT method achieves better modelling accuracy compared with the conventional DT recursive least square method. The effectiveness of the presented method for online SOC estimation is also verified on test data.

Keywords—Equivalent circuit model, continuous time domain estimation, linear integral filter method, parameter and SOC estimation, recursive least square.

I. INTRODUCTION

IN recent years, battery energy storage systems are being widely used in high power and high energy applications, such as electric vehicles (EVs) and power grid support. A battery model plays an important role for the system analysis, design, control and optimization. Equivalent circuit models (ECMs), which use a combination of electric components (resistors, capacitors etc., as shown in Fig. 1) to describe the battery terminal voltage and current (VI) dynamics, have been widely used for battery modelling and model-based state estimation, such as the state of charge (SOC) estimation [1]-[3]. The advantages of using ECMs are the simple model structure, low computational expense and acceptable accuracy.

One issue that needs to be taken into consideration when developing an ECM is that the battery performance changes with the working condition, such as the temperature and SOC levels. For example, at a typical mid-SOC value, the battery resistance is approximately doubled when the temperature drops from 25°C to 0°C [4]. The effect can be characterized offline and captured by using varying model parameters depending on the temperature and SOC [1], [4], [5]. On the other hand, the battery dynamics also change as the battery

ages, which may be a very slow process with a time duration of a few months and years and is very difficult to fully characterize offline. Similarly, the dependence of the model parameters on temperature and SOC may also change with the battery ageing, making the previous characterization obsolete. Therefore, online battery model parameter identification is necessary in order to capture the evolving nature of the battery behaviour in realtime, and to improve the accuracy.

Different methods for online battery ECM parameter identification have been proposed in the literature, which in general can be categorized into two groups, i.e., the recursive least square (RLS) method [6]-[12], and the Kalman filter (KF) method [13], [14]. Verbrugge [7] proposed an adaptive algorithm for online battery model parameter identification and SOC estimation using the RLS method. The governing equations of an ECM are formulated into a 'linear in the parameter (LITP)' way, so that the weighted RLS (WRLS) can be adopted for recursive parameter identification. The open circuit voltage (OCV) hysteresis effect is also considered in the model. Plett [13] proposed using joint extended Kalman filter (EKF) for the simultaneous estimation of the battery SOC and the time-varying model parameters. Duong et al. [11] proposed an online battery SOC and model parameter estimation method using the WRLS algorithm with multiple adaptive forgetting factors (FFs). Unlike the RLS method that uses only a single FF, multiple FFs are assigned to different model parameters that are varying at different rates. The algorithm is validated using test data on a LiFePO₄ battery cell, and shows improved modelling accuracy and parameter consistency. Hu [15] proposed a two time-scale scheme for online battery ECM parameter identification. The battery fast and slow dynamics are separated using a high-pass and a low pass filter, and thus the model parameters are divided and estimated separately.

Up to now, according to the authors' best knowledge, only discrete time (DT) identification methods have been used for online battery model parameter estimation, e.g., the widely used RLS method mentioned above. However, those DT methods have some limitations. One issue is the numerical difficulty due to the widely separated poles of the battery model. Another problem shows in the case of fast sampling because the model poles lie close to the unit circle in the complex domain, so that the model parameters are more poorly defined in statistical terms [16]. These problems can lead to poor estimation accuracy, or unreasonable estimation results, as illuminated in [11], [15]. These problems can

James Marco, Walid Allafi, Truong Q. Dinh and W. D. Widanage are with the Energy and Electrical Systems Group, Warwick Manufacturing Group, University of Warwick, Coventry, CV4 7AL, UK.

Cheng Zhang is with the Energy and Electrical Systems Group, Warwick Manufacturing Group, University of Warwick, Coventry, CV4 7AL, UK (Corresponding author; e-mail: c.zhang.11@warwick.ac.uk).

be circumvented using continuous time (CT) identification methods, which have several advantages over the DT methods. For example, the CT model parameters are independent of the sampling time, and the CT methods can deal with widely separated model poles [16]-[18]. Therefore, this paper presents a CT method, i.e., the linear integral filter (LIF) method, for online estimation of the battery ECM parameters, and it shows improved modelling accuracy compared with the DT RLS method using experimental data. The method can also be used for SOC estimation.

The reminder of this paper is organized as follows: Section II presents the battery model, and Section III introduces the DT RLS and CT LIF estimation methods. The battery test data and the experimental results are presented in Section IV, along with the result analysis and potential future research work. Finally Section V concludes this paper.

II. BATTERY ECM

A battery equivalent circuit model is shown in Fig. 1, where OCV is a function of battery SOC. v, i are the battery terminal voltage and current, respectively. R_i is the internal resistance. v_j is the over-potential across the j -th RC networks. The resistors and capacitors are usually the time-varying model parameters to be identified.

m is the total number of RC network, and $m = 2$ is usually a good trade-off between model accuracy and complexity [3]-[5], and thus is selected in this paper.

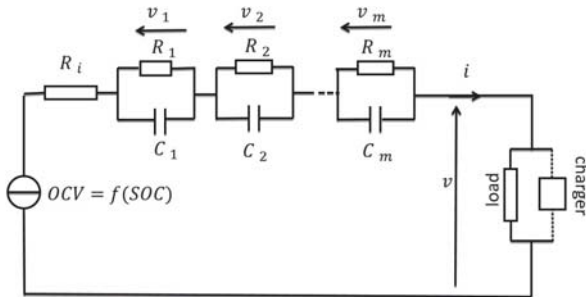


Fig. 1 A m -th order battery electric circuit model

The model equations are given as follows,

$$\begin{aligned} \frac{d}{dt} soc(t) &= \frac{1}{C_n} * i(t) \\ \frac{d}{dt} v_j(t) &= -a_j * v_j(t) + b_j * i(t), j = 1, 2, \dots, m \\ v(t) &= OCV(soc(t)) + \sum_{j=1}^m v_j(t) + R_i * i(t) \end{aligned} \quad (1)$$

where

$$a_j = \frac{1}{R_j C_j}, \quad b_j = 1/C_j$$

C_n is the battery capacity (unit: Ampere second).

Let $v_o = v - OCV = R_i * i + v_1 + v_2$, then from (1), yielding

$$v_o(t) = (R_i + \frac{b_1}{s + a_1} + \frac{b_2}{s + a_2}) * i(t) + c_0 \quad (2)$$

where s stands for the Laplace transform variable. Note that an extra constant c_0 is introduced to represent the OCV bias

caused by possible SOC initial error, as will be discussed in Section IV. Then we can get,

$$v_o^{(2)} = \theta_1 * v_o^{(1)} + \theta_2 * v_o + \theta_3 * i^{(2)} + \theta_4 * i^{(1)} + \theta_5 * i + \theta_6 \quad (3)$$

where $x^{(k)}$ stands for the k -th order derivative of the variable $x(t)$. The relationship between θ_j and a_j, b_j (or R_i, R_1, C_1, R_2, C_2) is straightforward and is omitted here.

III. CT LIF METHOD AND DT RLS METHOD

A. CT LIF Method

As it can be seen that (3) becomes a LITP problem if the time derivatives can be calculated. There are various ways of calculating the derivatives, such as linear filter methods, LIF methods, and modulating function methods, etc, and each method is characterized by specific advantages such as mathematical convenience, simplicity in numerical implementation and computation, physical insight, accuracy and others [16], [17]. The LIF method is selected here due to its ease of digital implementation and the elimination of extra burden of calculating initial conditions [17]. The LIF method, in this case, deals with the derivatives in (3) by performing two successive integral calculations on both sides of (3), i.e.,

$$\int_{t_2 - L * T_s}^{t_2} \int_{t_1 - L * T_s}^{t_1} (3) \quad dt dt_1 \quad (4)$$

where T_s the sampling time, L is a positive integral number, and thus $L * T_s$ is the time window of the integral calculation.

Define the time shifter q as $x(t - T_s) = q^{-1} * x(t)$, and the two functions [17],

$$f_1 = (1 - q^{-L})$$

$$f_2 = T_s * (0.5 + q^{-1} + q^{-2} + \dots + q^{-L+1} + 0.5 * q^{-L})$$

Then assume that first-order holder discretization method is used, yielding,

$$\int_{t-L * T_s}^t x(\tau) d\tau = f_2 * x(t)$$

$$\int_{t-L * T_s}^t x^{(1)}(\tau) d\tau = f_1 * x(t)$$

Then from (4), we can get

$$\begin{aligned} f_1^2 * v_o(t) &= \theta_1 * f_1 * f_2 * v_o(t) + \theta_2 * f_2^2 * v_o(t) \\ &+ \theta_3 * f_1^2 * i(t) + \theta_4 * f_1 * f_2 * i(t) \\ &+ \theta_5 * f_2^2 * i(t) + \theta_6 * T_s^2 * L^2 \end{aligned} \quad (5)$$

Let

$$y(t) = f_1^2 * v_o(t)$$

$$\phi(t) = [f_1 * f_2 * v_o(t), f_2^2 * v_o(t), f_1^2 * i(t), f_1 * f_2 * i(t), f_2^2 * i(t), L^2 * T_s^2]^T$$

then, (5) becomes

$$y(t) = \phi^T(t) * \theta + e(t) \quad (6)$$

where $\theta = [\theta_1, \dots, \theta_6]^T$, and $e(t)$ is introduced as the modelling error. This is a typical LITP problem, and the

parameters θ can be estimated recursively using the WRLS method, as follows.

$$\begin{aligned} e(t+1) &= y(t+1) - \phi^T(t+1)\theta(t) \\ \theta(t+1) &= \theta(t) + P(t+1)\phi(t+1)e(t+1) \\ P(t+1) &= \frac{1}{\lambda} \left(P(t) - \frac{P(t)\phi(t+1)\phi^T(t+1)P(t)}{\lambda + \phi^T(t+1)P(t)\phi(t+1)} \right) \end{aligned} \quad (7)$$

where λ is the FF. The initial parameters $\theta(0), P(0)$ can be obtained by performing a block-wise least square estimation.

B. DT RLS Method

Equation (2) can be discretized as follows,

$$v_o(t) = \frac{n_0 + n_1 * q^{-1} + n_2 * q^{-2}}{1 - d_1 * q^{-1} - d_2 * q^{-2}} * i(t) + c_0 \quad (8)$$

and then yielding,

$$v_o(t) = \phi_d^T(t) * \theta_d + e(t) \quad (9)$$

where

$$\begin{aligned} \phi_d(t) &= [v_o(t-T_s), v_o(t-2T_s), i(t), i(t-T_s), i(t-2T_s), 1]^T \\ \theta_d &= [d_1, d_2, n_0, n_1, n_2, -c_0 * (1 - d_1 - d_2)]^T \end{aligned}$$

$e(t)$ is the modelling error. This is again a LITP problem, and the WRLS method can be used.

There are some techniques to improve the parameter estimation stability and consistency of the WRLS method, such as data pre-processing (e.g., normalization), variable FF or directional forgetting, algorithm turn on/off scheme, covariance resetting [19]. Here the turn-on-turn-off method is adopted, namely, turning off the parameter adaption when the modelling error keeps low for a certain time period (e.g., $\frac{1}{N_1} * \sum_{\tau=t-N_1T_s}^t e^2(\tau) < e_{th}$ where e_{th} is the threshold level), and then turning on again when the error increases over the threshold. This is because the battery model parameters are assumed to change slowly (since the battery SOC or temperature usually change slowly), and if the modelling error keeps low, it is reasonable to assume that the optimal model parameters have been found. An upper-limit threshold value of the trace of $P(t)$ is also adopted to prevent covariance blowup [19] and unnecessary parameter fluctuations, as follows

$$\begin{aligned} \text{if } \text{trace}(P(t)) > P_{tr,max}, \\ \text{then } P(t) &= P(t) * P_{tr,max} / \text{trace}(P(t)) \end{aligned}$$

IV. EXPERIMENTAL RESULTS

A. Modelling Results

Two dynamic load test data sets are collected using a lithium ion NCA 18650 cell at the room temperature (25 °C), for model training and validation, as shown in Figs. 2 and 3, respectively. The sampling time is one second. The experimentally derived battery OCV versus SOC curve is shown in Fig. 4. This battery shows a low hysteresis effect [20], which is thus neglected. Only the test data between 20-90% SOC is used for the model training and validation to avoid the highly nonlinear zones of the battery dynamics. Usually lithium ion batteries are operated within this SOC

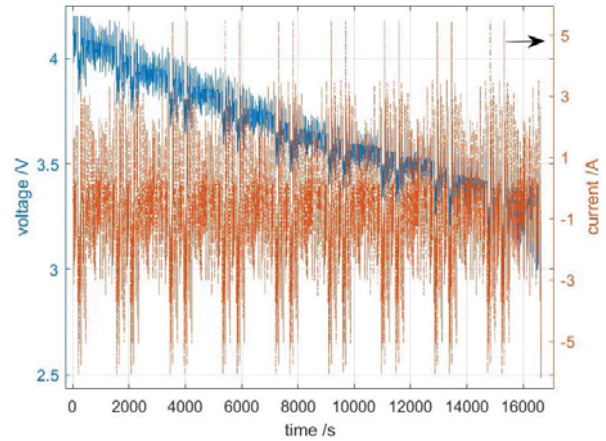


Fig. 2 Model training data set: test starts from 100% SOC till end of discharge

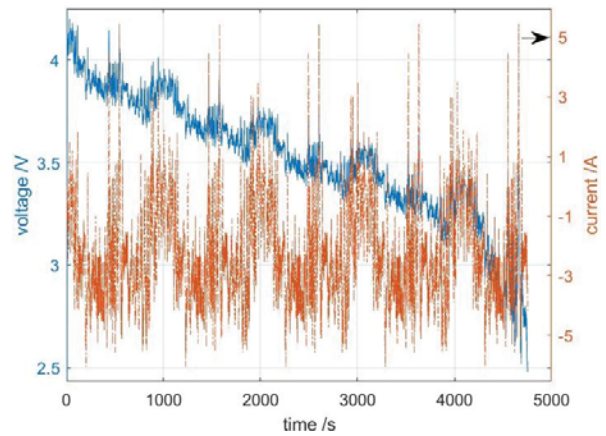


Fig. 3 Model validation data set: test starts from 100% SOC till end of discharge

range, because cycling operations at too high and too low SOC degrade the battery much faster [21].

The identified model parameters using the training data set are given in Figs. 5 and 6 for the CT LIF method and the DT RLS method, respectively, where $\tau_{oj} = R_j * C_j$ stands for the j -th RC network time constant. The two RC time constants of the CT model lie around 10s and 200s, respectively, and the two resistors R_1, R_2 are both significant. On the other hand, the DT model has one RC network (R_2C_2) with $\tau_{o2} \approx 0.5s, R_2 \approx 0.6m\Omega$, whose voltage contribution

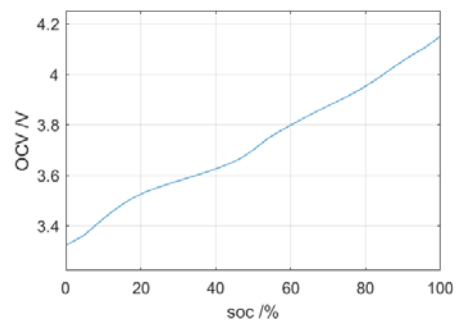


Fig. 4 Battery OCV vs SOC

is almost negligible compared with that of $R1C1$. Since the larger time constant of the DT model is about 20s, we assume that it has limited capacity of capturing battery low dynamics outside its frequency range, e.g., $< 0.01Hz$. In contrast, the CT model should be able to model the battery dynamics accurately at a wider frequency range compared with the DT model.

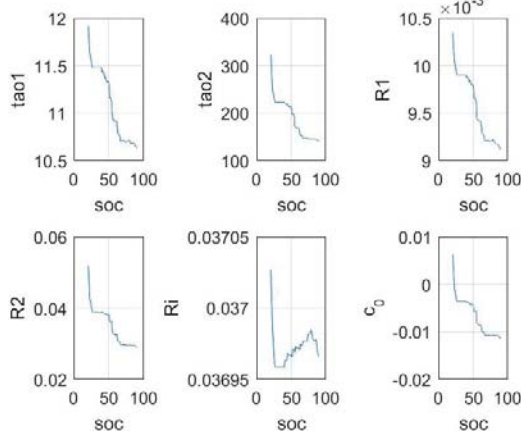


Fig. 5 Model parameter estimation results using CT LIF method on the training data set in Fig. 2

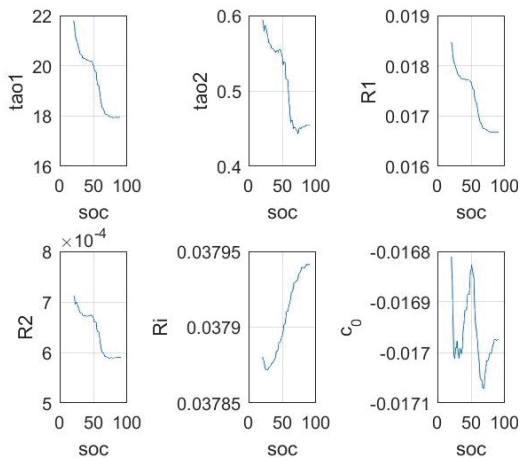


Fig. 6 Model parameter estimation results using DT RLS method on the training data set in Fig. 2

The model training errors are shown in Fig. 7, which shows the one-step-ahead (OSA) prediction error, i.e., $e(t)$ in (6) and (9). The results show that the DT and CT models produce similar OSA prediction accuracy. Since the OSA error weights lower on the low-frequency range and higher on the high-frequency range, the advantage of the CT model on the low frequency range is suppressed. To further compare between the CT and DT models, we run simulations using the identified DT and CT models on both the training and validation data set. The results are shown in Figs. 8 and 9, which clearly show that the CT model outperforms the DT model in terms of long term prediction accuracy. The simulation root mean square errors (RMSEs) using the training data set (in Fig. 8) are 21.6 mV and 36.3 mV for the CT and

DT method, respectively. The simulation RMSEs using the validation data set (in Fig. 9) are 17.3 mV and 53.8 mV for the CT and DT method, respectively.

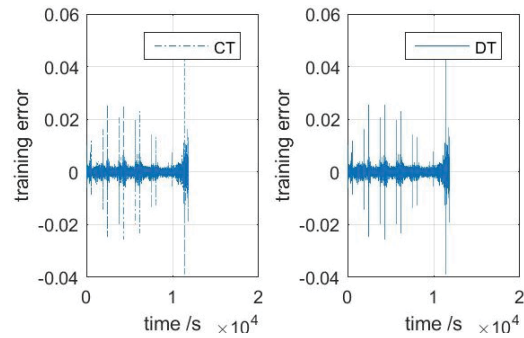


Fig. 7 Modelling error using CT LIF and DT RLS methods on the training data set in Fig. 2: OSA prediction error

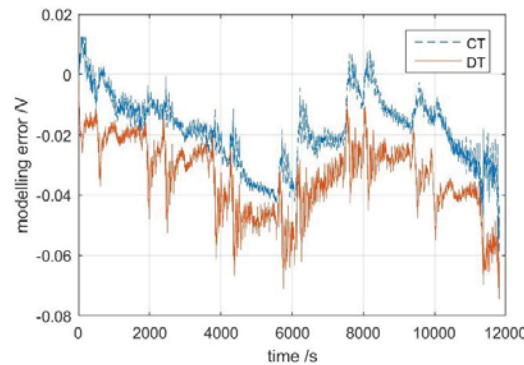


Fig. 8 Modelling error using CT LIF and DT RLS methods on the training data set in Fig. 2: simulation error

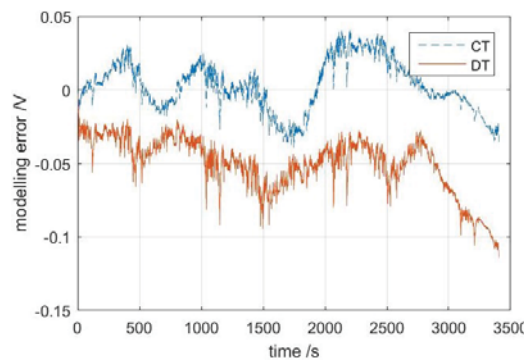


Fig. 9 Modelling error using CT LIF and DT RLS methods on the validation data set in Fig. 3: simulation error

B. SOC Estimation Results

The battery SOC is assumed to be known in the above analysis, then the battery OCV can be calculated using the OCV-SOC relationship, and then the calculation of $v_o = v - OCV$. In practise, there may exist an initial SOC estimation error. Assume a linear piecewise relationship between the battery OCV and SOC (which is valid according to Fig. 4), this initial SOC error will generate a constant bias in the

OCV estimation, i.e., c_0 in (2), which is a slowly time-varying constant depending on the SOC error and the slope of the OCV-SOC curve. Therefore, once this parameter c_0 is estimated, the battery OCV can be compensated as $OCV - c_0$, and then the battery SOC estimation can be corrected. Note that after this correction, the v_o values need to be updated to $v_o + c_0$, and then reset $c_0 = 0$. The rest model parameters can thus remain almost unaffected. This overall procedure is shown as follows,

First, initialize $soc(0), \theta(0), P(0)$. Then at time $t = kT$

- 1) measure voltage and current $v(t), i(t)$
- 2) update $soc(t)$ in (1)
- 3) calculate $OCV(t)$ using the OCV-SOC look-up table, and then calculate $v_o(t) = v(t) - OCV(t)$
- 4) calculate $y(t), \phi(t)$ in (6)
- 5) update $\theta(t), P(t)$ in (7)
- 6) compensate $OCV(t) = OCV(t) - c_0$; update $soc(t)$ using the OCV-SOC table. Then update $v_o(t - 2LT_s : t) = v_o(t - 2LT_s : t) + c_0$; then reset $c_0 = 0$. Note that the Matlab syntax is used here to indicate the way of variable update.

Note that the OCV compensation step 6) does not need to be implemented in every iteration. Actually, step 6 is implemented only when c_0 is stable and significant (large than a threshold value c_{th} corresponding to 2% SOC deviation), i.e.,

$$\frac{1}{N_2} \sum_{\tau=t-N_2T_s}^t c_0(\tau) > c_{th}$$

By means of an example, assume a 20% initial SOC error using the training data set, and run the above parameter and SOC estimation procedure, the SOC estimation results are given in Fig. 10. As it can be seen, the SOC estimation method can effectively correct the large initial error. The obtained SOC RMSE is about 2.3%.

C. Discussion and Future Work

From (2) and (8), it may be appealing to use the recursive instrumental variable (RIV) method [22], or recursive output error estimation method [23], rather than the RLS method for parameter identification. The adaption scheme of RIV method is more complex than the RLS method and more care needs to be taken for parameter convergence analysis. Further, the CT LIF method has already achieved desirable modelling accuracy, and thus the RIV method is not covered in this paper. However, this may constitute our future work.

The OCV hysteresis effect of the NCA cell used in this paper is negligible for SOC estimation. However, for other lithium ion cells, e.g., $LiFePO_4$ cell, the hysteresis effect needs to be taken into consideration in order to obtain accurate SOC estimation. This will be dealt with in our future work.

V. CONCLUSION

Battery ECMs are widely used in the battery management systems in EVs and other battery energy storage systems, and play a key role in the system analysis and control. The model parameters vary with the operating condition and thus need to

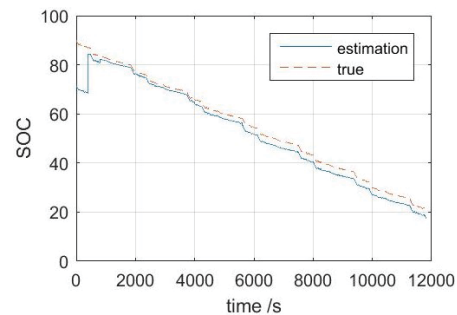


Fig. 10 SOC estimation results using CT LIF method on the training data set

be estimated in realtime to improve the modelling accuracy. This paper presents a new way of online ECM parameter estimation using the CT LIF method, which shows improved modelling accuracy compared with the conventional DT RLS method. The proposed method can also be used for online SOC estimation. Test data are collected on a lithium ion cell, and the experimental results have verified the effectiveness of the proposed method for both model parameter and SOC estimation.

ACKNOWLEDGMENT

The research was undertaken in collaboration with the WMG Centre High Value Manufacturing Catapult (funded by Innovate UK) and as a part of the ELEVATE project (EP/M009394/1) funded by the Engineering and Physical Science Research Council (EPSRC).

REFERENCES

- [1] M. Chen and G. A. Rincon-Mora, "Accurate electrical battery model capable of predicting runtime and IV performance," *Energy conversion, IEEE Transactions on*, vol. 21, no. 2, pp. 504–511, 2006.
- [2] G. L. Plett, "Extended kalman filtering for battery management systems of lipb-based HEV battery packs: Part 1. background," *Journal of Power Sources*, vol. 134, no. 2, pp. 252–261, 2004.
- [3] C. Zhang, K. Li, L. Pei, and C. Zhu, "An integrated approach for real-time model-based state-of-charge estimation of lithium-ion batteries," *Journal of Power Sources*, vol. 283, pp. 24–36, 2015.
- [4] C. Zhang, K. Li, J. Deng, and S. Song, "Improved realtime state-of-charge estimation of lifepo4 battery based on a novel thermoelectric model," *Industrial Electronics, IEEE Transactions on*, p. accepted, 2016.
- [5] W. Widanage, A. Barai, G. Chouchelamane, K. Uddin, A. McGordon, J. Marco, and P. Jennings, "Design and use of multisine signals for li-ion battery equivalent circuit modelling. part 2: Model estimation," *Journal of Power Sources*, vol. 324, pp. 61–69, 2016.
- [6] M. Verbrugge and E. Tate, "Adaptive state of charge algorithm for nickel metal hydride batteries including hysteresis phenomena," *Journal of Power Sources*, vol. 126, no. 1, pp. 236–249, 2004.
- [7] M. Verbrugge and B. Koch, "Generalized recursive algorithm for adaptive multiparameter regression application to lead acid, nickel metal hydride, and lithium-ion batteries," *Journal of The Electrochemical Society*, vol. 153, no. 1, pp. A187–A201, 2006.
- [8] H. Rahimi-Eichi, F. Baronti, and M.-Y. Chow, "Online adaptive parameter identification and state-of-charge coestimation for lithium-polymer battery cells," *IEEE Transactions on Industrial Electronics*, vol. 61, no. 4, pp. 2053–2061, 2014.
- [9] R. Xiong, F. Sun, X. Gong, and C. Gao, "A data-driven based adaptive state of charge estimator of lithium-ion polymer battery used in electric vehicles," *Applied Energy*, vol. 113, pp. 1421–1433, 2014.
- [10] H. He, X. Zhang, R. Xiong, Y. Xu, and H. Guo, "Online model-based estimation of state-of-charge and open-circuit voltage of lithium-ion batteries in electric vehicles," *Energy*, vol. 39, no. 1, pp. 310–318, 2012.

- [11] V.-H. Duong, H. A. Bastawrous, K. Lim, K. W. See, P. Zhang, and S. X. Dou, "Online state of charge and model parameters estimation of the lifepo4 battery in electric vehicles using multiple adaptive forgetting factors recursive least-squares," *Journal of Power Sources*, vol. 296, pp. 215–224, 2015.
- [12] Z. Wei, K. J. Tseng, N. Wai, T. M. Lim, and M. Skyllas-Kazacos, "Adaptive estimation of state of charge and capacity with online identified battery model for vanadium redox flow battery," *Journal of Power Sources*, vol. 332, pp. 389–398, 2016.
- [13] G. L. Plett, "Extended kalman filtering for battery management systems of lipb-based HEV battery packs: Part 3. state and parameter estimation," *Journal of Power sources*, vol. 134, no. 2, pp. 277–292, 2004.
- [14] —, "Sigma-point kalman filtering for battery management systems of lipb-based HEV battery packs: Part 2: Simultaneous state and parameter estimation," *Journal of Power Sources*, vol. 161, no. 2, pp. 1369–1384, 2006.
- [15] Y. Hu and Y.-Y. Wang, "Two time-scaled battery model identification with application to battery state estimation," *IEEE Transactions on Control Systems Technology*, vol. 23, no. 3, pp. 1180–1188, 2015.
- [16] H. Garnier, L. Wang, and P. C. Young, "Direct identification of continuous-time models from sampled data: Issues, basic solutions and relevance," in *Identification of continuous-time models from sampled data*. Springer, 2008, pp. 1–29.
- [17] H. Garnier, M. Mensler, and A. Richard, "Continuous-time model identification from sampled data: implementation issues and performance evaluation," *International Journal of Control*, vol. 76, no. 13, pp. 1337–1357, 2003.
- [18] H. Unbehauen and G. Rao, "A review of identification in continuous-time systems," *Annual reviews in Control*, vol. 22, pp. 145–171, 1998.
- [19] N. Rao Sripada and D. Grant Fisher, "Improved least squares identification," *International Journal of Control*, vol. 46, no. 6, pp. 1889–1913, 1987.
- [20] A. Barai, W. D. Widanage, J. Marco, A. McGordon, and P. Jennings, "A study of the open circuit voltage characterization technique and hysteresis assessment of lithium-ion cells," *Journal of Power Sources*, vol. 295, pp. 99–107, 2015.
- [21] A. Barré, B. Deguilhem, S. Grolleau, M. Gérard, F. Suard, and D. Riu, "A review on lithium-ion battery ageing mechanisms and estimations for automotive applications," *Journal of Power Sources*, vol. 241, pp. 680–689, 2013.
- [22] S. Sagara and Z.-Y. Zhao, "Numerical integration approach to on-line identification of continuous-time systems," *Automatica*, vol. 26, no. 1, pp. 63–74, 1990.
- [23] L. Dugard and I. Landau, "Recursive output error identification algorithms theory and evaluation," *Automatica*, vol. 16, no. 5, pp. 443–462, 1980.